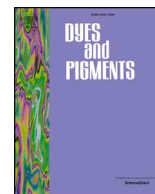




ELSEVIER

Contents lists available at ScienceDirect

Dyes and Pigments

journal homepage: www.elsevier.com/locate/dyepigNovel π -conjugated systems based on pyrimidine *N*-Oxide

Kseniya N. Sedenkova^{a,b}, Julia V. Kolodyazhnaya^a, Dmitry A. Vasilenko^a, Yulia A. Gracheva^a, Elena V. Kharitonoshvili^a, Yuri K. Grishin^a, Alexey A. Chistov^{c,d}, Victor B. Rybakov^a, Tina Holt^e, Andrei G. Kutateladze^e, Tamara S. Kuznetsova^a, Elena R. Milaeva^{a,b}, Elena B. Averina^{a,b,*}

^a Department of Chemistry, Lomonosov Moscow State University, Leninskie Gory, 1–3, Moscow, 119991, Russia

^b IPhAc RAS, Severnyi Proezd, 1, Chernogolovka, Moscow Region, 142432, Russia

^c Shemyakin-Ovchinnikov Institute of Bioorganic Chemistry, Miklukho-Maklaya 16/10, Moscow, 117997, Russia

^d Orekhovich Research Institute of Biomedical Chemistry, Pogodinskaya 10, Moscow, 119121, Russia

^e Department of Chemistry and Biochemistry, University of Denver, Denver, CO, 80208, USA

ARTICLE INFO

Keywords:

Pyrimidines
 π -Conjugated systems
 Knoevenagel condensation
 Fluorescence
 Metal cations
 Anticancer activity

ABSTRACT

Pyrimidine *N*-oxide moiety for the first time was used as a heterocyclic core for the construction of π -conjugated molecules with fluorescent properties. For the synthesis of the title compounds a simple two-step protocol starting from readily available 4-fluoro-2-methylpyrimidine *N*-oxides was elaborated. A series of 17 novel pyrimidine *N*-oxide derivatives containing various functional substituents and π -conjugated systems of different length were obtained. The title compounds revealed fluorescent properties in visible region, possessing emission maximum up to 575 nm. Deoxygenation of the *N*-oxide group led to the loss of visible fluorescence. The chemosensor properties towards TFA and a number of metal cations were demonstrated for **3a**, the first representative of the title series. Cytotoxic activity against breast adenocarcinoma cell line was found for three pyrimidine *N*-oxide derivatives **3b**, **i**, **n**. Pyrimidine *N*-oxide **3a** was shown to possess excellent biocompatibility and capability to enter cells, that makes it a promising structure for development of bioimaging fluorescent probes.

1. Introduction

Pyrimidine is an ubiquitous heterocyclic scaffold, particularly important in living organisms as a core of pyrimidine bases in nucleic acids, and also present in a number of drugs, including those with anticancer, antiviral, antibacterial and antihypertensive activities [1,2]. Another important application of aromatic strongly electron-withdrawing pyrimidine moiety is the construction of push-pull molecules and the synthesis of functionalized π -conjugated materials such as liquid crystals, light-emitting, and nonlinear optical materials [3]. The pyrimidine-based structures, containing simultaneously pharmacophore and fluorophore, are justifiably appealing for the development of bioimaging probes [4].

On contrary, pyrimidine *N*-oxides have been less investigated and found very few applications in pharmaceuticals or material sciences. The only clinical drug containing this scaffold is Minoxidil, an antihypertensive vasodilator medication used to treat hair loss [5]. Nevertheless, heterocyclic *N*-oxides possess their specific modes of action and represent highly challenging structures for drug-development

[6]. The use of pyrimidine *N*-oxides for construction of extended π -conjugated systems is not described either, despite having large electron-withdrawing effect and dipole moment, which is significantly higher than that of pyrimidines' [7]. The most evident cause of such oversight is the lack of straightforward and selective synthetic approaches to pyrimidine *N*-oxides and their functional derivatives.

Previously, we have discovered a three-component heterocyclization of 1,1-dihalogenocyclopropanes upon the treatment with nitrating or nitrosating reagents in the presence of an organic nitrile affording 4-halogenopyrimidine oxides (Scheme 1). Additionally, we elaborated approaches to a number of pyrimidine derivatives based on this reaction [8].

Here we present the synthetic approach to novel π -conjugated molecules based on pyrimidine *N*-oxide moiety and the investigation of their photophysical properties and anticancer activity.

* Corresponding author. Department of Chemistry, Lomonosov Moscow State University, Leninskie Gory, 1–3, Moscow, 119991, Russia.

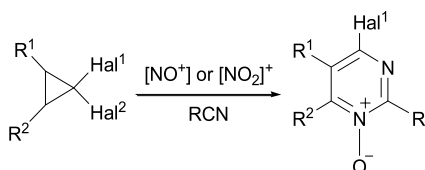
E-mail address: elaver@med.chem.msu.ru (E.B. Averina).

<https://doi.org/10.1016/j.dyepig.2018.12.067>

Received 6 November 2018; Received in revised form 26 December 2018; Accepted 30 December 2018

Available online 31 December 2018

0143-7208/© 2019 Elsevier Ltd. All rights reserved.



Scheme 1. Synthesis of 4-halogenopyrimidine *N*-oxides.

2. Materials and methods

2.1. Experimental

General. Heterocycles **1a,b**,^{8a,c} **2a-c**,^{8d} **5**^{8d} were obtained via described methods, synthesis and characterisation of novel intermediate compounds **1c**, **2d-f** are available in SI. All starting materials were commercially available. All reagents except commercial products of satisfactory quality were purified according to literature procedures prior to use. Analytical thin layer chromatography was carried out with silica gel plates (supported on aluminum); the detection was done by UV lamp (254 and 365 nm). Column chromatography was performed on silica gel (Merck, 230–400 mesh). ¹H, ¹³C and ¹⁹F NMR spectra were recorded on a 400 MHz spectrometer (400.0, 100.6 and 376.3 MHz for ¹H, ¹³C and ¹⁹F, respectively) at room temperature; chemical shifts were measured with reference to the solvent for [1]H (CDCl₃, δ = 7.24 ppm) and ¹³C (CDCl₃, δ = 77.13 ppm) and to CFCl₃ as external standard for ¹⁹F. When necessary, assignments of signals in NMR spectra were made using 2D techniques. Accurate mass measurements (HRMS) were obtained with electrospray ionization (ESI) and a time-of-flight (TOF) detector. Ultraviolet/Visible spectra were obtained on Agilent Cary 60 spectrophotometer. Fluorescence spectra in solutions were recorded on Hitachi F2700 fluorescence spectrophotometer. Fluorescence spectrum of **3a** in thin film was recorded on Fluoromax4 fluorescence spectrophotometer. Fluorescence quantum yield (± 10%) determined relative to quinine sulfate in 0.05 M H₂SO₄ (ψ = 53%) and rodamine-G in ethanol for **3o** (ψ = 94%) as standards [9]. Fluorescence intensity decays were obtained by time-correlated single photon-counting measurements in CH₂Cl₂ at 25 °C at c ≈ 10⁻⁵ M. Excitation wavelength – 370 nm. Typical fluorescence intensity decay data were analyzed by the Marquardt-Levenberg method of nonlinear fitting of one-, two- or three-exponential function (as a sum of discrete exponential terms); in the cases of **3a,o,q** not monoexponential intensity decay was observed.

2.2. Synthesis

Condensation of 4-aminopyrimidine oxides with aldehydes in basic conditions (general method). A mixture of 4-aminopyrimidine *N*-oxide **2** (0.5 mmol), corresponding aldehyde (1.0 mmol), 50% aqueous NaOH (2 g, 0.05 mol) and TEBAC (5 mg, 0.02 mmol) was stirred for 1–6 h under argon at 90–100 °C. After this time, the reaction mixture was allowed to cool down, diluted with water (5 mL) and extracted with CH₂Cl₂ (4 × 5 mL). The combined organic extracts were washed with water (3 × 5 mL) and dried over MgSO₄. The solvent was evaporated in vacuo and the product was isolated via the column chromatography (SiO₂).

Compound 3a was synthesized according to the general procedure (reaction time 1 h) from **2a** and benzaldehyde in 20% isolated yield. Yellow crystals, mp 185–188 °C (from CH₂Cl₂), Rf 0.3 (petroleum ether:EtOAc:MeOH 1:1:0.2). ¹H NMR (400.0 MHz, CDCl₃) δ_H: 1.65–1.75 (2H, m, C⁶H₂), 1.85–1.95 (2H, m, C⁷H₂), 2.59 (2H, m, C⁵H₂), 2.97 (m, 2H, C⁸H₂), 3.31–3.38 (4H, m, 2 CH₂N), 3.81–3.90 (4H, m, 2CH₂O), 7.29–7.39 (3H, m, 3CH, Ph), 7.62–7.68 (2H, m, 2CH, Ph), 7.90 (1H, br.d, J = 16.2 Hz, CH =), 7.99 (1H, d, J = 16.2 Hz, CH =); ¹³C NMR (100.6 MHz, CDCl₃) δ_C: 21.4 (C⁷H₂), 21.7 (C⁶H₂), 25.5 (CH₂), 26.3 (CH₂), 49.0 (2CH₂N), 66.7 (2CH₂O), 117.9 (CH =), 119.8 (C^{4a}),

127.9 (2CH, Ph), 128.7 (2CH, Ph), 129.3 (CH, Ph), 136.2 (C, Ph), 139.2 (CH =), 151.2 (C²), 154.5 (C⁴), 155.9 (C^{8a}). Found: [M + H]⁺ 338.1860; molecular formula C₂₀H₂₃N₃O₂ requires [M + H]⁺ 338.1863.

Compound 3b was synthesized according to the general procedure (reaction time 3 h) from **2a** and 2,6-dimethylbenzaldehyde in 32% isolated yield. Yellow crystals, mp 162–164 °C (from CH₂Cl₂), Rf 0.3 (petroleum ether:EtOAc:MeOH 1:1:0.2). ¹H NMR (400.0 MHz, CDCl₃) δ_H: 1.66–1.74 (2H, m, CH₂), 1.86–1.95 (2H, m, CH₂), 2.42 (6H, s, 2CH₃), 2.58 (2H, m, CH₂), 2.95 (2H, m, CH₂), 3.30–3.38 (4H, m, 2CH₂N), 3.80–3.88 (4H, m, 2CH₂O), 7.03–7.12 (3H, m, 3CH, Ar), 7.59 (1H, d, J = 16.5 Hz, CH =), 8.08 (1H, d, J = 16.5 Hz, CH =); ¹³C NMR (100.6 MHz, CDCl₃) δ_C: 21.3 (2CH₃), 21.4 (CH₂), 21.7 (CH₂), 25.4 (CH₂), 26.3 (CH₂), 49.0 (2CH₂N), 66.7 (2CH₂O), 119.8 (C^{4a}), 123.0 (CH =), 127.7 (CH, Ar), 128.2 (2CH, Ar), 135.3 (C, Ar), 136.8 (2C, Ar), 137.6 (CH =), 151.2 (C²), 154.4 (C⁴), 155.9 (C^{8a}). Found: [M + H]⁺ 366.2170; molecular formula C₂₂H₂₇N₃O₂ requires [M + H]⁺ 366.2176.

Compound 3c was synthesized according to the general procedure (reaction time 5 h) from **2a** and 4-methylbenzaldehyde in 25% isolated yield. Yellow crystals, mp 203–206 °C (from CH₂Cl₂), Rf 0.3 (petroleum ether:EtOAc:MeOH 1:1:0.2). ¹H NMR (400.0 MHz, CDCl₃) δ_H: 1.65–1.75 (2H, m, C⁶H₂), 1.86–1.96 (2H, m, C⁷H₂), 2.58 (2H, m, C⁵H₂), 2.95 (2H, m, C⁸H₂), 3.02 (6H, s, 2CH₃, NMe₂), 3.30–3.36 (4H, m, 2CH₂N), 3.83–3.89 (4H, m, 2CH₂O), 6.66–6.72 (2H, m, 2CH, Ar), 7.53–7.60 (2H, m, 2CH, Ar), 7.79 (1H, d, J = 16.1 Hz, CH =), 7.87 (d, 1H, J = 16.1 Hz, CH =); ¹³C NMR (100.6 MHz, CDCl₃) δ_C: 21.5 (C⁷H₂), 21.7 (C⁶H₂), 25.6 (C⁸H₂), 26.1 (C⁵H₂), 40.2 (2CH₃), 49.0 (2CH₂N), 66.8 (2CH₂O), 111.9 (2CH), 112.7 (=CH), 118.5 (C^{4a}), 124.3 (C, Ar) 129.5 (2CH), 139.7 (=CH), 151.1 (C, Ar), 152.0 (C²), 154.5 (C⁴), 155.5 (C^{8a}). Found: [M + H]⁺ 381.2285; molecular formula C₂₂H₂₈N₄O₂ requires [M + H]⁺ 381.2285.

Compound 3d was synthesized according to the general procedure (reaction time 6 h) from **2a** and 4-methoxybenzaldehyde in 27% isolated yield. Yellow crystals, mp 171–172 °C (from CH₂Cl₂), Rf 0.3 (petroleum ether:EtOAc:MeOH 1:1:0.2). ¹H NMR (400.0 MHz, CDCl₃) δ_H: 1.63–1.76 (2H, m, C⁶H₂), 1.84–1.94 (2H, m, C⁷H₂), 2.57 (2H, m, C⁵H₂), 2.96 (2H, m, C⁸H₂), 3.31–3.39 (4H, m, 2CH₂N), 3.80–3.87 (4H, m, 2CH₂O), 3.83 (3H, s, CH₃), 6.87–6.93 (m, 2H, 2CH, Ar), 7.57–7.63 (2H, m, 2CH, Ar), 7.84 (1H, d, J = 16.2 Hz, CH), 7.87 (1H, d, J = 16.2 Hz, CH =); ¹³C NMR (100.6 MHz, CDCl₃) δ_C: 21.4 (C⁷H₂), 21.7 (C⁶H₂), 25.5 (C⁸H₂), 26.3 (C⁵H₂), 49.0 (2CH₂N), 55.3 (CH₃), 66.7 (2CH₂O), 114.2 (2CH), 115.4 (=CH), 119.2 (C^{4a}), 128.9 (C, Ar) 129.5 (2CH), 139.2 (=CH), 151.6 (C²), 154.8 (C⁴), 155.8 (C^{8a}), 160.7 (C, Ar). Found: [M + H]⁺ 368.1962; molecular formula C₂₁H₂₅N₃O₃ requires [M + H]⁺ 368.1969.

Compound 3e was synthesized according to the general procedure (reaction time 6 h) from **2a** and 4-ethoxybenzaldehyde in 25% isolated yield. Yellow crystals, mp 166–169 °C (from CH₂Cl₂), Rf 0.2 (petroleum ether:EtOAc:MeOH 1:1:0.2). ¹H NMR (400.0 MHz, CDCl₃) δ_H: 1.41 (3H, t, J = 7.0 Hz, CH₃), 1.61–1.76 (2H, m, C⁶H₂), 1.83–1.94 (2H, m, C⁷H₂), 2.57 (2H, m, C⁵H₂), 2.95 (2H, m, C⁸H₂), 3.26–3.38 (4H, m, 2CH₂N), 3.79–3.88 (4H, m, 2CH₂O), 4.05 (2H, q, J = 7.0 Hz, CH₂, Et), 6.88 (2H, d, J = 8.6 Hz, 2CH), 7.58 (2H, d, J = 8.6 Hz, 2CH), 7.85 (2H, d, J = 16.2 Hz, 2CH =). ¹³C NMR (100.6 MHz, CDCl₃) δ_C: 14.8 (CH₃), 21.4 (C⁷H₂), 21.7 (C⁶H₂), 25.5 (C⁸H₂), 26.2 (C⁵H₂), 49.0 (2CH₂N), 63.5 (CH₂, Et), 66.7 (2CH₂O), 114.7 (2CH, Ar), 115.4 (CH =), 119.3 (C^{4a}), 128.8 (C), 129.5 (2CH, Ar), 139.0 (CH =), 151.5 (C²), 154.6 (C⁴), 155.8 (C^{8a}), 160.1 (C, Ar). Found: [M + H]⁺ 382.2116; molecular formula C₂₂H₂₇N₃O₃ requires [M + H]⁺ 382.2125.

Compound 3f was synthesized according to the general procedure (reaction time 6 h) from **2a** and 3,4,5-trimethoxybenzaldehyde in 15% isolated yield. Yellow crystals, mp 162–165 °C (from CH₂Cl₂), Rf 0.16 (petroleum ether:EtOAc:MeOH 1:1:0.2). ¹H NMR (400.0 MHz, CDCl₃) δ_H: 1.67–1.73 (2H, m, C⁶H₂), 1.85–1.96 (2H, m, C⁷H₂), 2.58 (2H, m, C⁵H₂), 2.95 (2H, m, C⁸H₂), 3.29–3.38 (4H, m, 2CH₂N), 3.82–3.87 (4H, m, 2CH₂O), 3.87 (3H, s, CH₃), 3.89 (6H, s, 2CH₃), 6.87 (2H, s, 2CH), 7.80 (1H, d, J = 16.0 Hz, CH =), 7.91 (1H, d, J = 16.0 Hz, CH =); ¹³C

NMR (100.6 MHz, CDCl₃) δ_C : 21.4 (C⁶H₂), 21.7 (C⁷H₂), 25.5 (C⁸H₂), 26.3 (C⁵H₂), 49.0 (2CH₂N), 56.2 (2CH₃), 60.9 (CH₃), 66.7 (2CH₂O), 105.0 (2CH), 117.2 (CH =), 119.8 (C^{4a}), 131.8 (C, Ar), 139.1 (CH =), 139.3 (C, Ar), 151.1 (C²), 153.4 (2C, Ar), 154.6 (C⁴), 155.9 (C^{8a}). Found: [M+H]⁺ 428.2169; molecular formula C₂₃H₂₉N₃O₅ requires [M+H]⁺ 428.2180.

Compound 3g was synthesized according to the general procedure (reaction time 6 h) from **2a** and 4-(diethoxymethyl)benzaldehyde. Was not isolated because of transformation into **3h** on silica gel. ¹H NMR (400.0 MHz, CDCl₃) δ_H : 1.25 (6H, t, *J* = 6.8 Hz, 2CH₃), 1.69–1.77 (2H, m, C⁶H₂), 1.88–1.97 (2H, m, C⁷H₂), 2.60 (2H, m, C⁵H₂), 3.00 (2H, m, C⁸H₂), 3.33–3.44 (4H, m, 2CH₂N), 3.51–3.69 (4H, m, 2CH₂, Et), 3.83–3.91 (4H, m, CH₂O), 5.52 (1H, s, CH), 7.50 (2H, d, *J* = 8.2 Hz, 2CH, Ar), 7.66 (2H, d, *J* = 8.2 Hz, 2CH), 7.92 (1H, d, *J* = 15.9 Hz, CH), 7.98 (1H, d, *J* = 15.9 Hz, CH).

Compound 3h was obtained from compound **3g** after the column chromatography in 12% isolated yield (per starting compound **2a**). Orange crystals, mp 186–188 °C (from CH₂Cl₂), R_f 0.5 (petroleum ether:EtOAc:MeOH 1:1:0.4). ¹H NMR (400.0 MHz, CDCl₃) δ_H : 1.66–1.74 (2H, m, C⁶H₂), 1.88–1.95 (2H, m, C⁷H₂), 2.59 (2H, m, C⁵H₂), 2.95 (2H, m, C⁸H₂), 3.29–3.38 (4H, m, 2CH₂N), 3.79–3.89 (4H, m, 2CH₂O), 7.78 (2H, d, *J* = 8.1 Hz, 2CH), 7.88 (2H, d, *J* = 8.1 Hz, 2CH), 7.92 (1H, d, *J* = 16.1 Hz, CH =), 8.10 (1H, d, *J* = 16.1 Hz, CH =), 10.0 (1H, s, CHO); ¹³C NMR (100.6 MHz, CDCl₃) δ_C : 21.3 (C⁷H₂), 21.6 (C⁶H₂), 25.5 (C⁸H₂), 26.3 (C⁵H₂), 49.0 (2CH₂N), 66.7 (2CH₂O), 120.7 (C^{4a}), 121.2 (=CH), 128.3 (2CH, Ar), 130.1 (2CH, Ar), 136.3 (C, Ar), 137.3 (=CH), 142.0 (C, Ar), 150.5 (C²), 154.5 (C⁴), 156.1 (C^{8a}), 191.6 (CHO). Found: [M+H]⁺ 366.1811; molecular formula C₂₁H₂₃N₃O₃ requires [M+H]⁺ 366.1812.

Compound 3i was synthesized according to the general procedure (reaction time 2 h) from **2a** and *trans*-4-stilbenecarboxaldehyde in 25% isolated yield. Yellow crystals, mp 188–191 °C (from CH₂Cl₂), R_f 0.2 (petroleum ether:EtOAc:MeOH 1:1:0.2). ¹H NMR (400.0 MHz, CDCl₃) δ_H : 1.65–1.74 (2H, m, C⁶H₂), 1.85–1.95 (2H, m, C⁷H₂), 2.59 (2H, m, C⁵H₂), 2.98 (2H, m, C⁸H₂), 3.32–3.40 (4H, m, 2CH₂N), 3.81–3.89 (4H, m, 2CH₂O), 7.09 (1H, d, *J* = 16.3 Hz, =CH), 7.16 (1H, d, *J* = 16.3 Hz, CH), 7.23–7.28 (1H, m, CH), 7.32–7.38 (2H, m, 2CH), 7.48–7.55 (4H, m, 4CH), 7.65 (2H, d, *J* = 8.3 Hz, 2CH), 7.90 (1H, d, *J* = 16.1 Hz, =CH), 8.01 (1H, d, *J* = 16.1 Hz, =CH); ¹³C NMR (100.6 MHz, CDCl₃) δ_C : 21.4 (C⁷H₂), 21.7 (C⁶H₂), 25.6 (C⁸H₂), 26.4 (C⁵H₂), 49.0 (2CH₂N), 66.7 (2CH₂O), 117.5 (CH =), 119.6 (C^{4a}), 126.6 (2CH), 126.9 (2CH), 127.8 (CH, Ph), 128.0 (CH =), 128.4 (2CH), 128.7 (2CH), 129.5 (CH =), 135.4 (C), 137.1 (C), 138.4 (C), 138.9 (CH =), 151.4 (C²), 154.9 (C⁴), 156.0 (C^{8a}). Found: [M+H]⁺ 440.2324; molecular formula C₂₈H₂₉N₃O₂ requires [M+H]⁺ 440.2333.

Compound 3j was synthesized according to the general procedure (reaction time 2 h) from **2b** and benzaldehyde in 17% isolated yield. Yellow oil, R_f 0.24 (petroleum ether: CH₂Cl₂:MeOH 3:1:0.1). ¹H NMR (400.0 MHz, CDCl₃) δ_H : 1.01 (3H, t, *J* = 7.3 Hz, CH₃), 1.46 (2H, m, CH₂, Bu), 1.67 (2H, m, CH₂, Bu), 1.73–1.86 (4H, m, C⁶H₂, C⁷H₂), 2.35 (2H, m, C⁵H₂), 2.95 (2H, m, C⁸H₂), 3.58 (2H, td, *J* = 7.0 Hz, *J* = 5.7 Hz, CH₂NH), 4.54 (1H, br.s, NH), 7.30–7.34 (1H, m, CH, Ph), 7.36–7.40 (2H, m, 2CH, Ph), 7.67 (2H, m, 2CH, Ph), 7.92 (1H, d, *J* = 16.1 Hz, CH =), 8.04 (d, 1H, *J* = 16.1 Hz, CH =); ¹³C NMR (100.6 MHz, CDCl₃) δ_C : 13.9 (CH₃), 20.2 (CH₂, Bu), 20.9 (C⁷H₂), 21.1 (C⁶H₂), 22.4 (C⁵H₂), 24.6 (C⁸H₂), 31.6 (CH₂, Bu), 41.0 (CH₂N), 112.8 (C^{4a}), 118.3 (CH =), 127.9 (2CH, Ph), 128.3 (CH, Ph), 128.7 (2CH, Ph), 136.4 (C, Ph), 138.8 (CH =), 151.3 (C⁴), 151.4 (C²), 153.4 (C^{8a}). Found: [M+H]⁺ 324.2068; molecular formula C₂₀H₂₅N₃O requires [M+H]⁺ 324.2070.

Compound 3k was synthesized according to the general procedure (reaction time 3 h) from **2c** and benzaldehyde in 21% isolated yield. Brown oil, R_f 0.2 (petroleum ether:EtOAc:MeOH 1:1:0.2). ¹H NMR (400.0 MHz, CDCl₃) δ_H : 1.85–1.90 (4H, m, C⁶H₂, C⁷H₂), 2.56 (2H, m, C⁵H₂), 3.00 (2H, m, C⁸H₂), 7.12–7.18 (2H, m, 2CH), 7.21–7.27 (1H, m, 1CH), 7.32–7.42 (4H, m, 4CH), 7.59–7.66 (3H, m, 3CH), 7.88 (1H, d, *J* = 16.0 Hz, CH =), 7.94 (1H, d, *J* = 16.0, CH =); ¹³C NMR

(100.6 MHz, CDCl₃) δ_C : 20.8 (C⁶H₂, C⁷H₂), 22.8 (C⁵H₂), 24.9 (C⁸H₂), 114.1 (C^{4a}), 117.4 (CH =), 120.9 (2CH), 124.0 (CH), 128.1 (2CH), 128.8 (2CH), 128.9 (2CH), 129.6 (CH), 135.9 (C, Ph), 138.4 (CH), 140.6 (C, Ph), 151.9 (C), 152.1 (C), 154.9 (C^{8a}). Found: [M+H]⁺ 344.1751; molecular formula C₂₂H₂₁N₃O requires [M+H]⁺ 344.1757.

Compound 3l was synthesized according to the general procedure (reaction time 3 h) from **2d** and benzaldehyde in 21% isolated yield. Brown crystals, mp 108–109 °C (from CH₂Cl₂), R_f 0.2 (petroleum ether:EtOAc:MeOH 1:1:0.3). ¹H NMR (400.0 MHz, CDCl₃) δ_H : 1.75–1.89 (4H, m, C⁶H₂, C⁷H₂), 2.50 (2H, m, C⁵H₂), 2.93 (2H, m, C⁸H₂), 3.81 (3H, s, CH₃), 6.53 (1H, s, NH), 6.88–6.93 (2H, m, 2CH, Ar), 7.26–7.37 (3H, m, 3CH, Ph), 7.47–7.52 (2H, m, 2CH, Ar), 7.55–7.59 (2H, m, 2CH, Ph), 7.81 (1H, d, *J* = 16.0 Hz, =CH), 7.97 (1H, d, *J* = 16.0 Hz, =CH); ¹³C NMR (100.6 MHz, CDCl₃) δ_C : 20.9 (C⁶H₂), 21.0 (C⁷H₂), 22.7 (C⁵H₂), 24.9 (C⁸H₂), 55.5 (CH₃), 113.7 (C^{4a}), 114.0 (2CH, Ar), 117.9 (CH =), 122.8 (2CH, Ar), 127.9 (2CH, Ph), 128.7 (2CH, Ph), 129.2 (CH, Ph), 131.8 (C, Ar), 136.2 (C, Ph), 139.4 (CH =), 148.4 (C⁴), 151.3 (C²), 154.5 (C^{8a}), 156.1 (C, Ar). Found: [M+H]⁺ 374.1852; molecular formula C₂₃H₂₃N₃O₂ requires [M+H]⁺ 374.1863.

Compound 3m was synthesized according to the general procedure (reaction time 3 h) from **2a** and cinnamic aldehyde in 17% isolated yield. Yellow oil, R_f 0.4 (petroleum ether:EtOAc:MeOH 1:1:0.1). ¹H NMR (400.0 MHz, CDCl₃) δ_H : 1.62–1.76 (2H, m, C⁶H₂), 1.80–1.93 (2H, m, C⁷H₂), 2.58 (2H, m, C⁵H₂), 2.95 (2H, m, C⁸H₂), 3.29–3.37 (4H, m, 2CH₂N), 3.80–3.89 (4H, m, 2CH₂O), 7.31–7.40 (4H, m, 3CH, Ph, CH =), 7.44–7.50 (1H, m, CH =), 7.62–7.67 (2H, m, 2CH, Ph), 7.89 (1H, ps.d, *J* = 16.3 Hz, CH =), 7.98 (1H, ps.d, *J* = 16.0 Hz, CH =); ¹³C NMR (100.6 MHz, CDCl₃) δ_C : 21.4 (CH₂), 21.6 (CH₂), 25.5 (CH₂), 26.3 (CH₂), 49.0 (2CH₂N), 66.7 (2CH₂O), 117.8 (CH =), 119.7 (C^{4a}), 127.0 (CH =), 128.0 (2CH, Ph), 128.5 (CH =), 128.7 (2CH, Ph), 129.3 (CH, Ph), 136.1 (C, Ph), 139.3 (=CH), 151.2 (C²), 154.7 (C⁴), 156.0 (C^{8a}). Found: [M+H]⁺ 364.2017; molecular formula C₂₂H₂₅N₃O₂ requires [M+H]⁺ 364.2020.

Compound 3n was synthesized according to the general procedure (reaction time 2 h) from **2a** and 2-naphthaldehyde in 15% isolated yield. Orange crystals, mp 155–156 °C (from CH₂Cl₂), R_f 0.4 (petroleum ether:EtOAc:MeOH 1:1:0.2). ¹H NMR (400.0 MHz, CDCl₃) δ_H : 1.63–1.75 (2H, m, C⁶H₂), 1.83–1.94 (2H, m, C⁷H₂), 2.58 (2H, m, C⁵H₂), 2.97 (2H, m, C⁸H₂), 3.30–3.42 (4H, m, 2CH₂N), 3.80–3.90 (4H, m, 2CH₂O), 7.46–7.51 (2H, m, 2CH, Ar), 7.53–7.57 (1H, m, 1CH, Ar), 7.82–7.86 (2H, m, 2CH, Ar), 7.96 (1H, d, *J* = 7.1 Hz, CH, Ar), 8.05 (1H, d, *J* = 15.8 Hz, CH =), 8.23 (1H, d, *J* = 8.4 Hz, CH, Ar), 8.78 (1H, d, *J* = 15.8 Hz, CH =); ¹³C NMR (100.6 MHz, CDCl₃) δ_C : 21.4 (C⁷H₂), 21.7 (C⁶H₂), 25.5 (C⁸H₂), 26.3 (C⁵H₂), 49.0 (2CH₂N), 66.7 (2CH₂O), 120.0 (C^{4a}), 120.2 (CH =), 123.4 (CH, Ar), 124.9 (CH, Ar), 125.7 (CH, Ar), 125.9 (CH, Ar), 126.5 (CH, Ar), 128.7 (CH, Ar), 129.6 (CH, Ar), 131.5 (C, Ar), 133.3 (C, Ar), 133.7 (C, Ar), 135.8 (CH =), 151.2 (C²), 154.6 (C⁴), 156.0 (C^{8a}). Found: [M+H]⁺ 388.2010; molecular formula C₂₄H₂₅N₃O₂ requires [M+H]⁺ 388.2020.

Compound 3o was synthesized according to the general procedure (reaction time 5 h; 0.7 eq. of aldehyde were taken instead of 2 eq.) from **2a** and perylene-3-carboxaldehyde in 10% isolated yield. Dark-red crystals, mp 155–156 °C (from CH₂Cl₂), R_f 0.4 (petroleum ether:EtOAc:MeOH 1:1:0.4). ¹H NMR (400.0 MHz, CDCl₃) δ_H : 1.68–1.78 (2H, m, C⁶H₂), 1.88–1.97 (2H, m, C⁷H₂), 2.61 (2H, m, C⁵H₂), 2.99 (2H, m, C⁸H₂), 3.36–3.43 (4H, m, 2CH₂N), 3.85–3.92 (4H, m, 2CH₂O), 7.45–7.49 (2H, m, 2CH), 7.56 (1H, dd, *J* = 7.8, 8.4 Hz, CH), 7.65–7.69 (2H, m, 2CH), 7.98 (1H, d, *J* = 8.1 Hz, CH), 8.08 (1H, d, *J* = 15.7 Hz, =CH), 8.09 (1H, d, *J* = 8.4 Hz, CH), 8.22 (1H, d, *J* = 7.8 Hz, CH) 8.17–8.21 (3H, m, 3CH), 8.73 (1H, d, *J* = 15.7 Hz, =CH); ¹³C NMR (100.6 MHz, CDCl₃) δ_C : 21.4 (C⁷H₂), 21.7 (C⁶H₂), 25.5 (C⁸H₂), 26.3 (C⁵H₂), 49.1 (2CH₂N), 66.8 (2CH₂O), 119.7 (=CH), 119.9 (C^{4a}), 120.3 (CH), 120.4 (CH), 120.6 (CH), 120.8 (CH), 123.1 (CH), 125.7 (CH), 126.6 (CH), 126.7 (CH), 126.9 (CH), 128.0 (CH), 128.2 (CH), 128.4 (C), 129.0 (C), 130.9 (C), 131.2 (C), 131.7 (C), 132.5 (C), 132.7 (C), 132.9 (C), 134.6 (C), 135.4 (=CH), 151.3 (C²), 154.6 (C⁴),

156.0 (C^{8a}). Found: [M+H]⁺ 512.2326; molecular formula C₃₄H₂₉N₃O₂ requires [M+H]⁺ 512.2333.

Compound 3p was synthesized according to the general procedure (reaction time 6 h) from **2a** and thiophene-2-carboxaldehyde in 12% isolated yield. Yellow crystals, mp 130–131 °C (from CH₂Cl₂), R_f 0.2 (petroleum ether:EtOAc:MeOH 1:1:0.2). ¹H NMR (400.0 MHz, CDCl₃) δ_H: 1.64–1.75 (2H, m, C⁶H₂), 1.86–1.94 (2H, m, C⁷H₂), 2.57 (2H, m, C⁵H₂), 2.94 (2H, m, C⁸H₂), 3.29–3.36 (4H, m, 2CH₂N), 3.81–3.86 (4H, m, 2CH₂O), 7.03 (1H, dd, *J* = 3.7 Hz, *J* = 5.1 Hz, CH, Thio), 7.27 (1H, d, *J* = 3.7 Hz, CH, Thio), 7.32 (1H, d, *J* = 5.1 Hz, CH, Thio), 7.76 (1H, d, *J* = 15.8 Hz, CH =), 8.03 (1H, d, *J* = 15.8, CH =); ¹³C NMR (100.6 MHz, CDCl₃) δ_C: 21.4 (C⁷H₂), 21.7 (C⁶H₂), 25.5 (C⁸H₂), 26.2 (C⁵H₂), 49.0 (2CH₂N), 66.7 (2CH₂O), 117.1 (CH =), 119.6 (C^{4a}), 127.4 (CH, Thio), 127.9 (CH, Thio), 129.2 (CH, Thio), 131.7 (CH =), 141.9 (C, Thio), 150.9 (C²), 154.5 (C⁴), 155.8 (C^{8a}). Found: [M+H]⁺ 344.1426; molecular formula C₁₈H₂₁N₃O₂S requires [M+H]⁺ 344.1427.

Compound 3q was synthesized according to the general procedure (reaction time 1 h; 10% aqueous NaOH (0.7 g, 17.5 mmol) was taken instead of 50%) from **2e** and benzaldehyde in 19% isolated yield. Yellow crystals, mp 195–198 °C (from CH₂Cl₂), R_f 0.6 (petroleum ether:EtOAc:MeOH 1:1:0.3). ¹H NMR (400.0 MHz, CDCl₃) δ_H: 3.66–3.73 (4H, m, 2CH₂N), 3.79–3.89 (4H, m, 2CH₂O), 6.50 (1H, s, C⁵H), 7.31–7.41 (3H, m, 3CH, Ph), 7.42–7.49 (3H, m, 3CH, Ph), 7.63–7.68 (2H, m, 2CH, Ph), 7.74–7.78 (2H, m, 2CH, Ph), 7.93 (1H, d, *J* = 16.1 Hz, CH =), 8.03 (1H, d, *J* = 16.1 Hz, CH =); ¹³C NMR (100.6 MHz, CDCl₃) δ_C: 44.6 (2CH₂N), 66.4 (2CH₂O), 102.1 (C⁵H), 117.68 (CH =), 128.1 (2CH, Ph), 128.2 (2CH, Ph), 128.8 (2CH, Ph), 129.3 (2CH, Ph), 129.7 (CH, Ph), 130.2 (CH, Ph), 132.1 (C, Ph), 135.8 (C, Ph), 141.3 (CH =), 153.5 (C⁴), 155.3 (C²), 156.0 (C⁶). Found: [M+H]⁺ 360.1697; molecular formula C₂₂H₂₁N₃O₂ requires [M+H]⁺ 360.1707.

Compound 3r was synthesized according to the general procedure (reaction time 1 h; 10% aqueous NaOH (0.7 g, 17.5 mmol) was taken instead of 50%) from **2e** and benzaldehyde in 18% isolated yield. Yellow crystals, mp 210–212 °C (from CH₂Cl₂), R_f 0.7 (petroleum ether:EtOAc:MeOH 1:1:0.2). ¹H NMR (400.0 MHz, CDCl₃) δ_H: 3.64–3.69 (4H, m, 2CH₂N), 3.81–3.87 (4H, m, 2CH₂O), 6.49 (1H, s, C⁵H), 7.33–7.41 (3H, m, 3CH, Ph), 7.56–7.60 (2H, m, 2CH, C₆H₄Br), 7.63–7.67 (2H, m, 2CH, Ph), 7.69–7.73 (2H, m, 2CH, C₆H₄Br), 7.92 (1H, d, *J* = 16.1 Hz, CH =), 8.04 (1H, d, *J* = 16.1 Hz, CH =); ¹³C NMR (100.6 MHz, CDCl₃) δ_C: 44.6 (2CH₂N), 66.4 (2CH₂O), 101.9 (C⁵H), 117.7 (CH =), 124.7 (CBr), 128.1 (2CH, Ph), 128.8 (2CH, Ph), 129.6 (CH, Ph), 130.9 (2CH, C₆H₄Br), 131.1 (C, C₆H₄Br), 131.4 (2CH, C₆H₄Br), 135.8 (C, Ph), 140.8 (CH =), 152.5 (C⁴), 154.2 (C⁶), 154.9 (C²). Found: [M+H]⁺ 438.0821 and 440.0795; molecular formula C₂₂H₂₀BrN₃O₂ requires [M+H]⁺ 438.0812 and 440.0792.

Compound 4 was obtained from *N*-oxide **3a** via described method [8b] in 95% isolated yield and required no purification. Yellowish crystals, mp 113–114 °C (from CH₂Cl₂). ¹H NMR (400.0 MHz, CDCl₃) δ_H: 1.66–1.75 (2H, m, C⁶H₂), 1.80–1.89 (2H, m, C⁷H₂), 2.51 (2H, m, C⁵H₂), 2.83 (2H, m, C⁸H₂), 3.35–3.47 (4H, m, 2CH₂N), 3.74–3.85 (4H, m, 2CH₂O), 7.09 (1H, d, *J* = 16.0 Hz, =CH), 7.23–7.28 (1H, m, 1CH), 7.29–7.35 (2H, m, 2CH), 7.53–7.57 (2H, m, 2CH), 7.80 (1H, d, *J* = 16.0 Hz, CH); ¹³C NMR (100.6 MHz, CDCl₃) δ_C: 22.3 (C⁷H₂), 22.8 (C⁶H₂), 26.7 (C⁵H₂), 31.7 (C⁸H₂), 48.6 (2CH₂N), 66.8 (2CH₂O), 116.4 (C^{4a}), 127.4 (2CH), 127.6 (CH =), 128.61 (CH), 128.64 (2CH), 136.3 (C, Ph), 136.5 (CH =), 160.1 (C²), 164.2 (C^{8a}), 164.9 (C⁴). Found: [M+H]⁺ 322.1905; molecular formula C₂₀H₂₃N₃O requires [M+H]⁺ 322.1914.

2.3. X-ray analysis

For X-ray diffraction analysis was chosen single crystal of compound **3b**. Cell parameters for compound **3b** were determined from a set of 13467 reflections. Structure was solved by direct methods (SHELXS97) [10a], and refined with using anisotropic approximation for all

nonhydrogen atoms. All hydrogen atoms were found from the different Fourier maps and refined with using riding model. Refinement procedure was made with using SHELXL-13 program [10b]. The description and results of the single crystal experiment are given in Table S1. Graphical representations (Fig. S1) of solved molecular structure was made with using ORTEP-3 program [10c]. The CIF-file was checked (on-line procedure) by PLATON [10d] program and deposited in Cambridge Structural Data Base (deposit number 1545819). In the crystal structure classical hydrogen bonds are not found (Fig. S2). By our opinion, crystal structure is stabilized by non-classical hydrogen bonds (Table S3) and intermolecular contacts (less than 4.00 Å) (Table S4).

2.4. Computational details

Molecular modelling, with Gaussian 09 and GaussView 5.0.8, was used to determine the HOMO and LUMO energies at the B3LYP/6-31G(d) was performed. The theoretical calculations for excitation and emission spectra were carried out using the Gaussian 09 implementations of B3LYP DFT. Using the optimized geometries in CH₂Cl₂ (PCM model), vertical transitions in the UV–vis region were computed with time-dependent DFT (TDDFT) to generate the simulated absorption spectra. For TDDFT single points, the first 6 (for **3o** NState = 20) singlet excitations were solved iteratively [TD(ROOT = X, NSTATES = 6) where X is the root number, X = 1]. For TDDFT geometry optimizations, the first singlet excited states were optimized using analytical gradients, and the first 6 singlet excitations were solved iteratively [TD (ROOT = 1, NSTATES = 6)]. All Gaussian 09 computations used the 6-31G(d) basis sets for all atoms. Spherical harmonic d functions were used throughout, i.e., there are five angular basis functions per d function. All B3LYP/6-31G(d) structures were fully optimized, and analytical frequency calculations were performed on all ground-state structures to ensure a local minimum was achieved.

2.5. Bioevaluation

2.5.1. MTT test

The MTT test of compounds **3a-f,h,i,m-o** was performed according to the described procedure [11] with small modifications. MCF7, HCT116 human cancer cell lines were cultured in DMEM (PanEco, Russia) with Glutamin (PanEco, Russia) and antibiotics (PanEco, Russia) in CO₂ (5%) at 37 °C. The compounds were predissolved (20 mM) in DMSO and then added to the cell-culture medium at the required concentration with a maximum DMSO content of 0.5 v/v-%. At these concentrations, DMSO has no effect on cell viability, as it was shown in control experiments. Cells were cultured in 96-well plates (7000 cells/well) and treated with various concentrations of the title compounds (from 0.01 to 50 μM) as well as doxorubicin at 37 °C for 72 h. Cell viability was determined by using the MTT assay, which quantifies the mitochondrial activity. Then, the cells were incubated at 37 °C for 50 min with a solution of MTT, 3-(4,5-dimethylthiazol-2-yl)-2,5-diphenyltetrazolium bromide (10 μL, 5 mg × mL⁻¹) (Sigma-Aldrich, St. Louis, USA). The supernatant was discarded, and cells were dissolved in DMSO (100 μL). The optical density of the solution was measured at 570 nm with use of a multiwell-plate reader (Anthos Zenyth 2000rt, Biochrom, Great Britain), and the percentage of surviving cells was calculated from the absorbance of untreated cells. Each experiment was repeated at least three times, and each concentration was tested in at least three replicates. Data were presented as (relative cell growth inhibition) a graph of the percentage of surviving cells versus the concentration of the test substances (Fig. S4). The meanings of 50% inhibition concentration (IC₅₀) were performed with standard deviation.

2.5.2. Cell toxicity assay

The cytotoxicity of compounds **3a,c,e,f,i,j,l,n,q,r** was evaluated

according to the described procedure [12a]. The porcine embryo kidney (PEK) cell line were seeded and incubated at 37 °C for 72 h in 96-well plates. Stock solutions of the studied compounds with a concentration of 5 mM were prepared in 100% DMSO and two-fold dilutions were prepared in medium 199 in Earle solution to obtain final concentrations starting from 50 μ M. Equal volumes of compound dilutions were added in four replicates to the cells. Control cells were treated with the same sequential concentrations of DMSO, as in compound dilutions in four replicates in the same medium. After incubation at 37 °C on days 1 or 7, the morphology of the cells was visualized with the microscope and CC₅₀ values were calculated according to the Kerber method [12b].

2.5.3. Cell uptake behavior

The cell uptake behavior of compounds **3a** and **3n** was examined by a microscope AxioPlan 2 imaging MOT (Carl Zeiss, Germany) with a digital camera AxioCam Hrc (Carl Zeiss); photos were processed with AxioVision 4.5 soft (Carl Zeiss). HCT116 and MCF7 cells cultures (5×10^4 cells per mL) were used. The fluorescence was excited by a mercury lamp with FRET CFP filters (Filter set 48 FRET CFP/YFP shift free; EX BP 436/20, BS FT 455, EM BP 535/30). The cells were cultivated in flasks 72, unhitched and suspended in DMEM. Compounds **3a** or **3n** in concentrations 25 or 250 μ M were incubated with cells for 1 h at 25 °C. Afterward, the cells were washed two times with DMEM and the photos were obtained (Fig. 6, S6,7).

Synthetic details, characterisation of novel starting and intermediate compounds **1c**, **2d-f**, details of X-ray data collection and structure refinement, details of bioevaluation, copies of absorption and emission spectra, computational details, copies of NMR spectra are available in SI.

3. Results and discussions

Two main synthetic transformations were used for the approach to previously unknown π -conjugated systems: i) S_NAr reactions in electron-deficient pyrimidine oxide system and ii) the Knoevenagel-type condensation, employing methyl group in the position 2 of heteroaromatic ring [13]. It should be noted that in contrast with pyrimidines, the reactivity of the oxidized heterocycles had not been studied systematically. There is only one described example with the use of 2-methylpyrimidine oxides' condensation with an aldehyde [14a]; along with several examples of the synthesis of 2-ethenyl derivatives of pyrimidine oxide via heterocyclization^{14b-d} or oxidation [14e]. Furthermore, a limited number of examples of S_NAr reactions involving these compounds exists as well [8d,15]. Nevertheless, they definitely present promising substrates for such processes due to significant electron-withdrawing effect of the *N*-oxide moiety [7a,16].

The series of pyrimidine *N*-oxides **2a-f** bearing alkyl- or arylamino group in position 4 were obtained from pyrimidine *N*-oxides **1a-c** under the treatment with corresponding nucleophiles (Scheme 2). The reactions proceeded smoothly in mild conditions.

Amino substituted pyrimidine *N*-oxide **2a** was studied in condensation with benzaldehyde (Scheme 2). The optimization of condensation conditions, including varying of basic or acidic catalyst, solvent and temperature (Table S1), was carried out and in all cases the condensation proceeded selectively at the methyl group. The best result was achieved when 50% aqueous NaOH was used as a base in the presence of TEAC without organic solvent.

Under the optimized conditions, the series of novel pyrimidine *N*-oxides derivatives **3a-r** were obtained (Scheme 2). The aromatic aldehydes, containing electron donating substituents, were readily involved in the reaction with **2a** to give 2-arylidene pyrimidine *N*-oxides **3a-f, i-l**. Aldehydes containing the nitro-group or halogen atoms in the aryl moiety did not react with 2-methylpyrimidine *N*-oxides, and neither did acetophenone. The only condensation product containing an acceptor substituent in the styryl moiety that we obtained was compound **3h**. For

this purpose, *N*-oxide **3g** was prepared as the precursor. As a bonus no additional synthetic procedure was necessary because the acetal protective group was removed in the course of column chromatography.

The cinnamic aldehyde and aldehydes, containing naphthyl, perylenyl or thiophenyl moieties, reacted with *N*-oxide **2a** affording compounds **3m-p** (Scheme 2). Pyrimidine *N*-oxides **2e,f** were also involved into the reaction with benzaldehyde to give the heterocycles **3q,r** with an additional aryl moiety in the pyrimidine ring (Scheme 2). Diluted solution of NaOH was used because the starting compounds were both more reactive and more labile than tetrahydroquinazoline derivatives **2a-d**.

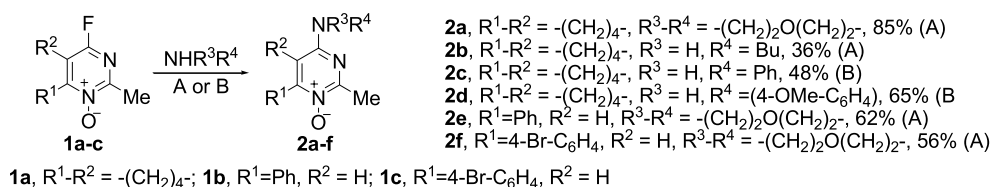
The product of *N*-oxide reduction in compound **2a**, pyrimidine **5**, was also studied in condensation with benzaldehyde, but proved to be inert under the reaction conditions (Scheme 3). Therefore, a better pathway to compound **4** is the reduction of condensation product **3a**. Such a difference in reactivity of pyrimidines and more electron-withdrawing pyrimidine *N*-oxides have been previously observed [14a] and showed the significance of *N*-oxide electronic effects for the chemical behavior of pyrimidine derivatives. Here, the comparison of **2a** and **5** in the condensation conditions demonstrates that the introduction of an *N*-oxide moiety into the molecule is sufficient to compensate for the deactivating effect of alkylamino group.

The photophysical properties of the obtained compounds were studied by UV-vis and fluorescence spectroscopy in CH₂Cl₂ at RT. Spectra of electronic absorption and emission were recorded; the absorption coefficients and fluorescence quantum yields were measured for all the obtained compounds (Fig. 1, Table 1).

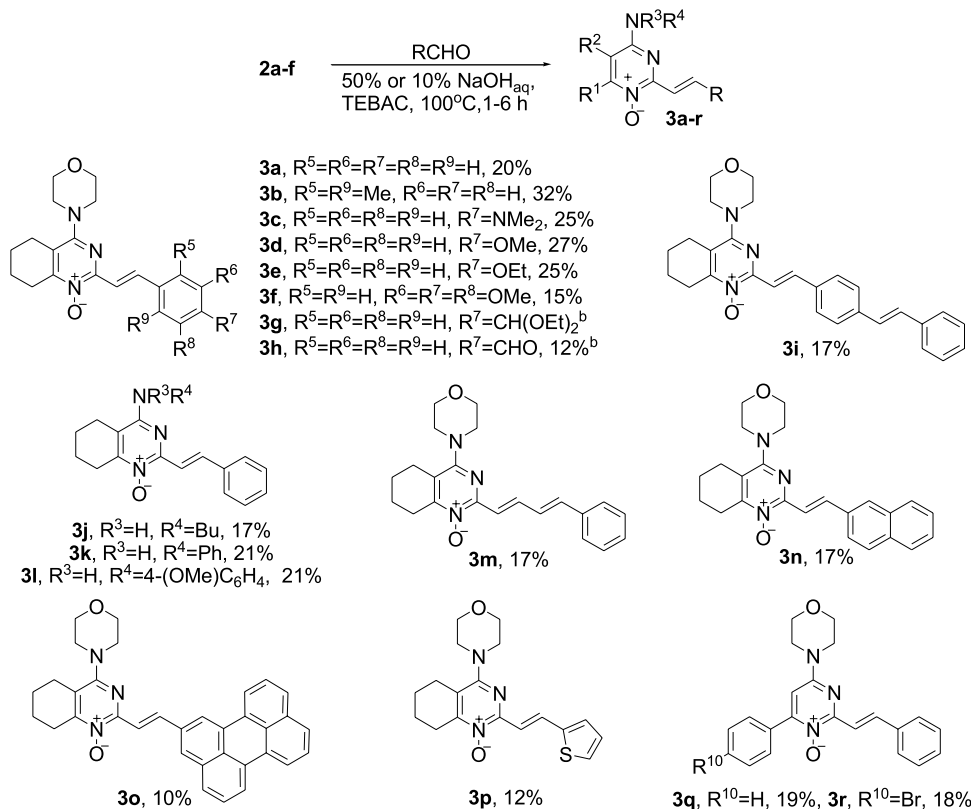
For most of the obtained compounds, the longest-wavelength absorption maxima are in the visible region, at 380–450 nm (Fig. 1, Table 1). The most significant red-shift of maxima relative to compound **3a** ($\lambda_{\text{abs}}^{\text{max}} = 400$ nm) was achieved when the six-membered ring annelated to the pyrimidine moiety was substituted for aryl (**3q,r**, $\lambda_{\text{abs}}^{\text{max}} = 445$ nm), or when the perylenyl moiety was introduced into the molecule (**3o**, $\lambda_{\text{abs}}^{\text{max}} = 470$ nm). Strong absorption (ϵ over $10^3 \text{ M}^{-1} \cdot \text{cm}^{-1}$) in the long-wave region was demonstrated by compounds **3i,n,o**, containing the extended systems of conjugated bonds. The largest hyperchromic effect was observed when dimethylamino group was introduced in the structure (**3c**, $\epsilon = 33 \cdot 10^3 \text{ M}^{-1} \cdot \text{cm}^{-1}$).

An interesting effect of structure on the absorption was observed for compound **3b**. Due to steric hindrance introduced by the *ortho*-methyl groups, the aryl ring is rotated out of the plane containing the pyrimidine moiety and double bond; whereas in **3a**, two aromatic rings lay in the same plane, and more effective conjugation is achieved. As a result, $\lambda_{\text{abs}}^{\text{max}}$ of dimethyl substituted compound **3b** is blueshifted comparing to **3a**. The molecular structure and geometry of **3b** were proved with DFT-calculations (for **3a,b**, Fig. S3) and X-ray analysis (for **3b**, Fig. S3).

π -Conjugated compounds **3a-r**, containing *N*-oxide moiety, were found to possess fluorescence properties in visible region. For compounds **3a-f**, either unsubstituted or bearing electron-donating groups in the aromatic ring, the emission maxima lay in the range of 515–536 nm (Fig. 1, Table 1). However, introduction of an aldehyde function in *p*-position of the phenyl fragment (**3h**) redshifts the longest-wavelength emission maximum up to $\lambda_{\text{em}}^{\text{max}} = 565$ nm. For 4-alkyl and 4-arylamino *N*-oxides **3j-l** the emission maxima are blueshifted, and the Stokes shift is smaller. Unlike with **3a**, this is caused by less electron-donative properties of the substituents (i.e as compared with the dialkylamino group). Extension of the π -system (compounds **3i,m,n,q,r**) redshifts the emission maxima considerably, and this effect is the strongest for perylenyl substituted compound **3o**, giving $\lambda_{\text{em}}^{\text{max}} = 575$ nm. Replacement of phenyl with thiophenyl in **3p** slightly increases emission maximum, but the quantum yield becomes appreciably lower, possibly because of a more efficient intersystem crossing into the triplet state due to the heavy atom effect. For the compound **3a** it was shown that in solid state there was no shift of the emission maximum. Fluorescence lifetimes were measured for the compounds



Conditions. **A**: morpholine or NH₂Bu as solvent, 24 h; **B**: NH₂Ph or NH₂(4-OMe-C₆H₄), DIPEA, EtOH, 1-7 days



Scheme 2. Synthesis of π -conjugated heterocycles based on pyrimidine *N*-oxides. (^aisolated yields; ^bacetal protective group of **3g** was removed on SiO₂ affording **3h**).

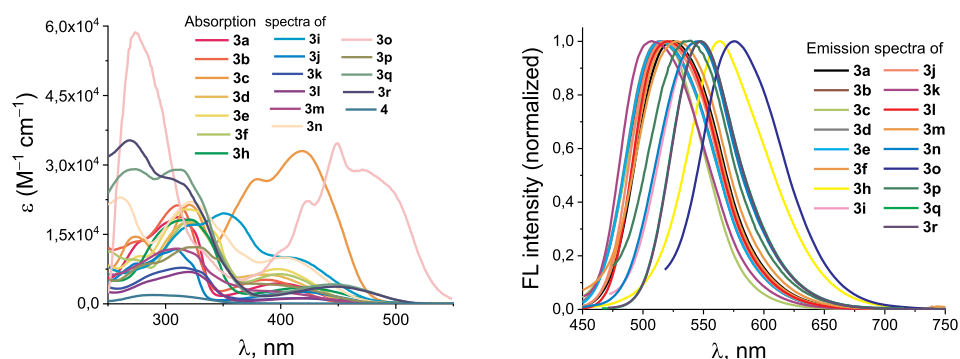
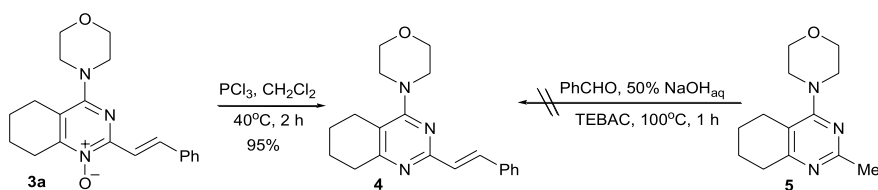


Table 1
Photophysical properties of compounds **3a–r**, **4**^a.

| | $\lambda_{\text{abs}}^{\text{max}}$, nm ^b | $\lambda_{\text{em}}^{\text{max}}$, nm | $\Delta\lambda$, cm ⁻¹ | ϵ , 10 ³ ·M ⁻¹ ·cm ⁻¹ | ψ , % | τ , ns | μ , D ^c |
|-----------|---|---|------------------------------------|---|------------|--------------------------------------|------------------------|
| 3a | 400 | 535 ^d | 6308 | 4.4 | 21 | 9.2 | 4.00 |
| 3b | 384 | 536 | 7385 | 5.2 | 29 | 9.1 | 4.53 |
| 3c | 420 | 523 | 4689 | 33.0 | 1.0 | – | 1.95 |
| 3d | 391 | 533 | 6814 | 6.3 | 12 | 8.3 | 2.02 |
| 3e | 384 | 515 | 6624 | 7.5 | 21 | 8.2 | 1.73 |
| 3f | 390 | 521 | 6447 | 6.4 | 23 | 8.5 | 6.14 |
| 3h | 418 | 565 | 6224 | 3.5 | 2.5 | – | 8.62 |
| 3i | 406 | 531 | 5798 | 10.0 | 4 | – | 3.67 |
| 3j | 415 | 520 | 4866 | 2.6 | 20 | 8.9 | 6.70 |
| 3k | 416 | 508 | 4353 | 1.2 | 16 | 1.7 (6%) 10.3 (94%) | 5.53 |
| 3l | 420 | 520 | 4579 | 4.3 | 13 | 8.2 | 7.39 |
| 3m | 400 | 546 | 6685 | 2.7 | 6 | – | 3.51 |
| 3n | 400 | 546 | 6685 | 10.0 | 5 | – | 3.79 |
| 3o | 470 | 575 | 3885 | 29.0 | 4 | 3.2 (69%) 5.4 (31%) | 3.92 |
| 3p | 400 | 534 | 6273 | 4.0 | 0.6 | – | 3.30 |
| 3q | 445 | 548 | 4224 | 4.2 | 20 | 0.7 (25%) 2.5 (42%) 10.7 (33%) | 4.26 |
| 3r | 445 | 548 | 4224 | 3.7 | 15 | 3.7 | 4.93 |
| 4 | 284 | 333 | 5181 | 1.9 | 2.3 | – | 2.52 |

^a All spectra were recorded in CH₂Cl₂ solutions at RT at $c = (1.0\text{--}6.0) \times 10^{-5}$ M.

^b The longest-wavelength absorption maxima.

^c Calculated dipole moments.

^d In solid state $\lambda_{\text{em}}^{\text{max}} = 537$ nm.

with the highest quantum yields, being in most cases 8–9 ns. A mono-exponential decrease in fluorescence was usually observed, but in some cases (especially if the molecule contained several aromatic rings) the dependence had a more complex form. Significant differences in fluorescence decay for **3q** and **3r** are apparently due to the presence of a bromine atom in the molecule.

Both the absorption and emission maxima of compound **4** were observed in UV region, being significantly blueshifted in comparison with its oxidized analogue **3a**. So, it can be concluded that the presence of *N*-oxide group is essential for the absorption and fluorescence in the visible part of the spectrum.

To gain a deeper understanding of the electronic and photophysical properties of the synthesized compounds, we performed quantum-chemical simulations for **3a–r** and **4**. The FMO plots show that the HOMOs of the *N*-oxide molecules are mainly localized in the aminopyrimidine moiety, while LUMOs are localized through the whole conjugated system (Fig. 2). Much less active charge-transfer is observed for deoxygenated analogue **4**, possessing strongly blueshifted

absorption and emission maxima. The dipole moments of the molecules were also predicted, giving 1.6–8.7 D (Table 1), yet no correlation was found between them and photophysical properties of pyrimidine *N*-oxides. Computational details, FMO plots and energies, and comparison of experimental and calculated absorption and emission maxima wavelengths are given in SI.

The investigated compounds possess solvatochromic effect, and for most of them, change in the emission color can be seen by the naked eye. Thus, for compound **3h**, changing the solvent from CH₂Cl₂ to methanol led to the change of fluorescence from yellow to green; that is presumably related to the formation of hydrogen bonds between carbonyl group and solvent molecules in methanol (Fig. 3).

Basing on their structure, the investigated compounds may be expected to exhibit aggregation-induced emission (AIE) feature [17]. In the search for the AIE effect, the emission spectra in CH₃CN–water with different volumetric ratios of water were recorded for the compound **3a**. It was shown (Fig. 4a and b) that the increase of solvent polarity leads to the hypsochromic shift of absorption and emission maxima; yet

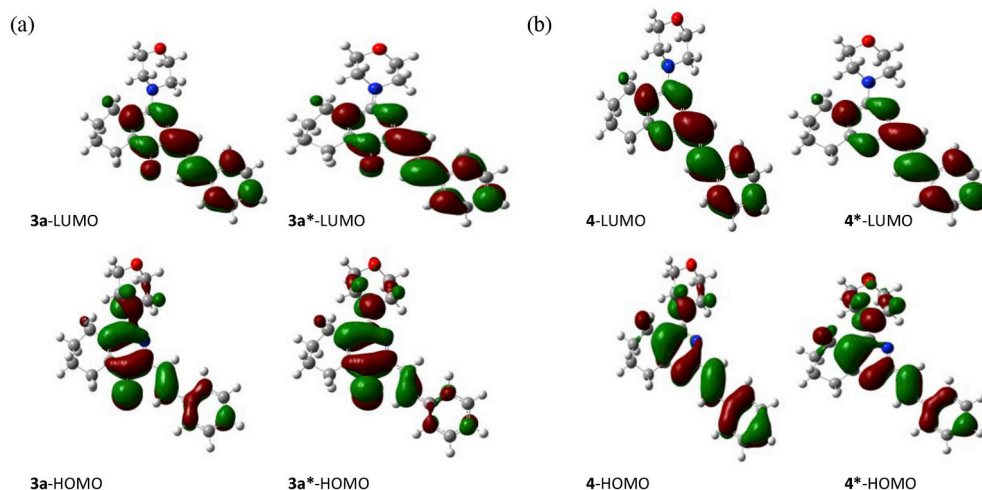


Fig. 2. FMO plots (B3LYP/6-31G(d)) of (a) **3a** and (b) **4** in ground and excited states. FMO plots of **3b–r** are shown in Figs. S10–S27 in the SI.

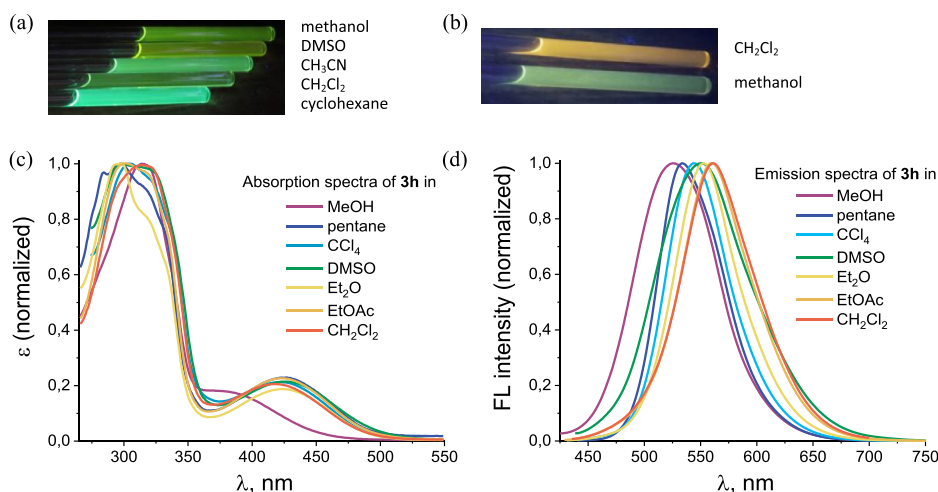


Fig. 3. Fluorescence of **3a** (a) and **3h** (b); absorption (c) and emission (d) spectra of **3h** in different solvents at RT, $\lambda_{\text{ex}} = 365$ nm.

neither AIE nor ACQ effects were observed.

For compound **3a**, the effect of the presence of acid in the medium on the absorption and fluorescence spectra was also studied. Upon addition of TFA, the absorption band at 400 nm disappeared and the solution of heterocycle became colorless. Fluorescent properties of **3a** were found to be sensitive to the medium pH: the protonation of the molecule led to fluorescence quenching (Fig. 4c and d).

To probe the chemosensor properties of compound **3a**, its absorption and emission spectra were investigated in the presence of the metal cations in various concentrations (Fig. 5). Analogous to the addition of acids, the addition of salts led to discoloration of the solution and significant quenching of fluorescence. There was no shift of wavelength maxima observed. The strongest changes were observed for Pb²⁺, Cu²⁺, Zn²⁺ ions, while Hg²⁺, Ag⁺, K⁺ ions showed almost no effect on absorption and emission (Fig. 5, S9).

It should be mentioned that such behavior is not common for

diazine fluorophores [**3a-c**]; the more common occurrence is the shift of emission bands upon protonation or complexation. Together with the lack of fluorescence in deoxygenated compound **4** it probably indicates that the proton or metal ion binding involves the N-oxide, not the heterocyclic moiety. To prove this suggestion DFT calculations were performed for different protonated forms of **3a**, where a proton was either bonded with a heteroatom or underwent an electrophilic addition to the C-C double bond. According to the calculations, the cationic form where the proton is bonded with the oxygen atom lays 3.11 kcal/mol lower than the next alternative form. During such a protonation the FMOs of **3a** have changed to those revealing no charge-transfer and strongly resembling the corresponding FMOs in non-fluorescent compound **4** (Fig. 2, S28). Speaking in terms of the electrons redistribution, the electron lone pair on oxygen of protonated **3a** is bonded with a proton and cannot participate in charge-transfer on contrast to the free **3a**. The same effect can be assumed in the case of metals ions

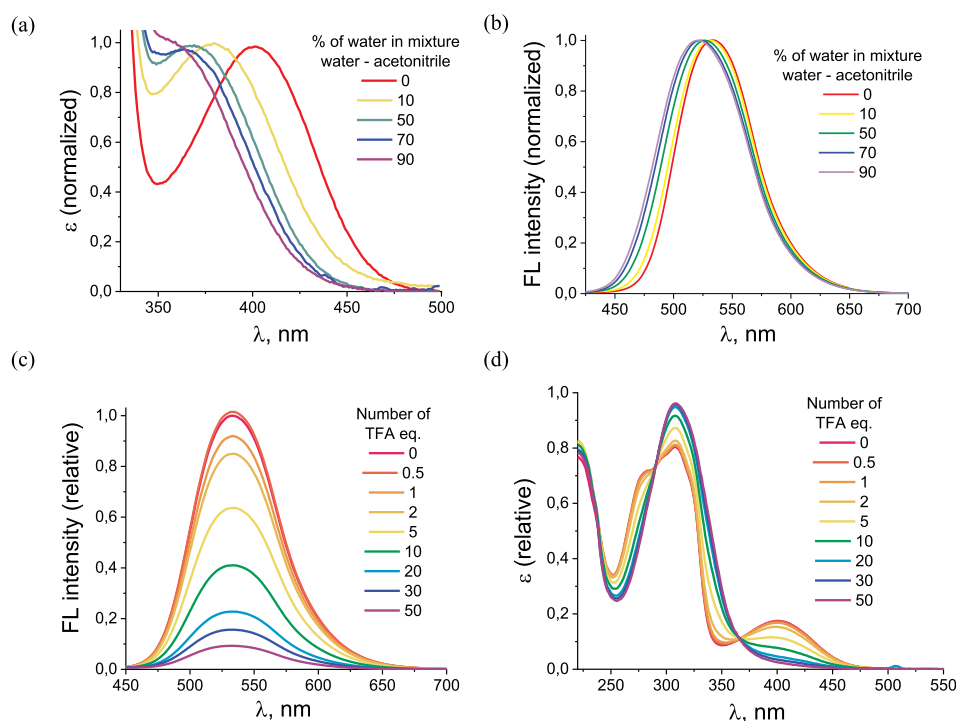


Fig. 4. Electronic absorption and fluorescence spectral change of **3a** (2×10^{-5} mol L⁻¹) at RT (a,b) in CH₃CN–water mixtures with varying volumetric fractions of water; (c,d) in CH₂Cl₂ upon addition of TFA; $\lambda_{\text{ex}} = 400$ nm.

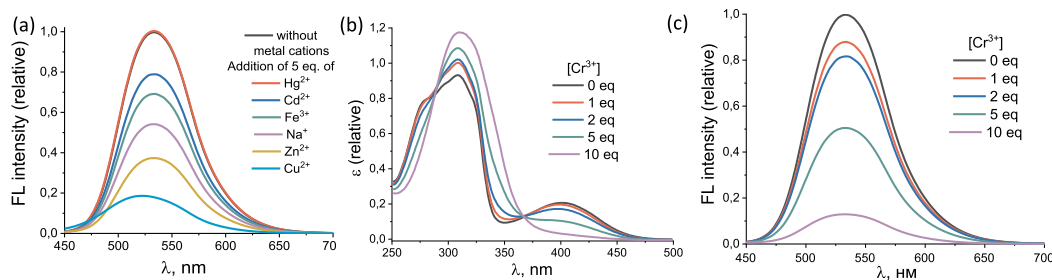


Fig. 5. (a) Fluorescence spectra of **3a** ($2 \times 10^{-5} \text{ mol L}^{-1}$) upon addition of Hg^{2+} , Cd^{2+} , Fe^{3+} , Na^+ , Zn^{2+} and Cu^{2+} (5 equiv.); (b,c) electronic absorption and fluorescence spectral change of **3a** ($2 \times 10^{-5} \text{ mol L}^{-1}$) upon addition of $\text{Cr}(\text{ClO}_4)_3$ in acetonitrile at RT; $\lambda_{\text{ex}} = 400 \text{ nm}$.

complexation that is to some extent confirmed by the pyrimidine *N*-oxides capability to bind with metals involving just oxygen, shown by X-ray analysis for the complex of **1a** with Cu^{2+} [8a].

To evaluate potential applications of the obtained pyrimidine *N*-oxides as leading compounds for drug development and fluorescent dyes for biological imaging [18] we investigated their antiproliferative activity towards human cancer cells, toxicity and the cell uptake behavior.

The primary screening of biological activity of the series of morpholine-substituted π -conjugated molecules was completed. Compounds **3a-f,h,i,m-o** were evaluated for their antitumor potency against 2 types of human cancer cell lines: colon carcinoma HCT-116 and breast adenocarcinoma MCF7 (Table 2).

Three of these compounds showed moderate cytotoxic activity against the MCF7 cancer cell line (IC_{50} values for **3b,i,n** are below $50 \mu\text{M}$), and the most active of them, compound **3n**, also demonstrated cytotoxicity towards the line HCT116 in micromolar concentration. Thus, in the studied series, the compound with the naphthalene moiety **3n** shows higher activity against both cell lines, which makes it the most promising candidate. This evaluation, though preliminary, reveals that introduction of hydrophobic sterically hindered substituents in position 2 is favorable for cytotoxicity.

The toxicity of a series of the pyrimidine oxides **3** was also investigated using the porcine embryo kidney (PEK) cell line. It was shown that **3a**, displaying no antiproliferative activity, also showed no acute (24 h) or chronic (7 d) toxicity in the concentrations up to of $50 \mu\text{M}$. Compound **3n**, on contrary, was found to be quite toxic, possessing $\text{CC}_{50} < 6.25 \mu\text{M}$. In the terms of selectivity it was shown **3i** to be more promising, as it revealed no acute (24 h) toxicity up to of $50 \mu\text{M}$, nevertheless it possessed $\text{CC}_{50} = 9.2 \pm 3.1 \mu\text{M}$.

For compounds **3a**, which have shown no cytotoxic activity, and **3n**, found to be the most active species, the cell uptake behavior on MCF7 and HCT116 cell lines was investigated and visualized. After incubation with $25 \mu\text{M}$ or $250 \mu\text{M}$ of a pyrimidine *N*-oxide for 1 h the cells were excited and the pictures were obtained (Fig. 6). Both compounds **3a** and **3n** were shown to be readily accumulated in cells. No difference was observed for active and inactive compounds that testifies that the lack of cytotoxicity of **3a** is not connected with its ability to enter the cell. Two investigated cancer cell lines showed no notable difference in the cell uptake either. The growth of the **3a** or **3n** concentration in the

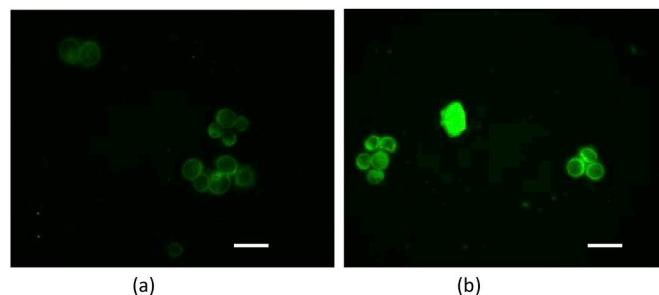


Fig. 6. Fluorescence of compound **3n** in MCF7 cells after incubation for 1 h. Concentration of **3n** was $25 \mu\text{M}$ (a) or $250 \mu\text{M}$ (b).

medium led to the fluorescence enhancement, probably, due to further accumulation of the substances inside the cells. Intensive fluorescence of the cells contour may point to the predominant accumulation of the pyrimidine oxides **3a,n** in cell membrane due to their hydrophobic properties.

Thus, depending on the substituents in the position 2 of the pyrimidine moiety the compounds **3** may possess significantly varying biological activity. Pyrimidine *N*-oxide **3a** possesses excellent biocompatibility and is capable to enter cells, that makes it a promising structure for development of bioimaging fluorescent probes, while antiproliferative activity found for **3b,i,n** and selectivity, shown by **3i**, allow to expect that further structural modification will lead to the structures, combining fluorescent properties, anticancer activity and high therapeutic index.

4. Conclusions

In summary, we have investigated a series of 2-methyl substituted pyrimidine *N*-oxides, bearing the substituents of various electronic nature, in the reaction with aromatic aldehydes. Basing on the studied reaction, the preparative approach to novel π -conjugated systems, containing pyrimidine *N*-oxide core, was elaborated and a series of previously unknown push-pull molecules were synthesized. Their photophysical properties were examined and it was found that all compounds possess the emission maxima more than 500 nm (up to 575 nm for compound **3o**, containing a perylenyl moiety). This redshift together with the either biocompatibility or antitumor activity, found for some of the obtained conjugated molecules, makes them promising compounds for various bioapplications.

Acknowledgements

We thank the Russian Foundation for Basic Research (project 18-03-00651-a) for financial support of this work. This study was fulfilled using a STOE STADI VARI PILATUS-100K diffractometer and NMR spectrometer Agilent 400-MR purchased by MSU Development Program. The research is supported in part by the National Science

Table 2

IC_{50} values for cell viability found for compounds **3b,i,n** and doxorubicin (Dox) against cancer cell lines.

| Compounds | IC_{50} , μM | |
|-----------|----------------------------------|-----------------|
| | HCT-116 | MCF7 |
| 3b | > 50 | 28.7 ± 8.4 |
| 3i | > 50 | 11.7 ± 4.3 |
| 3n | 8.6 ± 1.9 | 2.9 ± 0.5 |
| Dox | 0.65 ± 0.1 | 0.28 ± 0.06 |

Foundation, CHE-1665342. MTT-test is made with the financial support of the Russian Science Foundation (grant No. 14-03-00483). Authors thank Prof. Yuri V. Fedorov for the providing fluorescence life-time determination and discussions.

Appendix A. Supplementary data

Supplementary data to this article can be found online at <https://doi.org/10.1016/j.dyepig.2018.12.067>.

References

- [1] For reviews see.
 (a) Rewcastle GW, Katritzky AR, Ramsden CA, Scriven EFV, Taylor RJK, editors. *Comprehensive heterocyclic chemistry III*, vol. 8. Oxford: Elsevier Ltd.; 2008. p. 120;
 (b) Baumann M, Baxendale IR. *Beilstein J Org Chem* 2013;9:2265;
 (c) Prachayasittikul S, Pingaew R, Worachartcheewan A, Sinthupoom N, Prachayasittikul V, Ruchirawat S, Prachayasittikul V. *Mini Rev Med Chem* 2017;17:869
- [2] For recent examples see.
 (a) Beesu M, Salyer ACD, Brush MJH, Trautman KL, Hill JK, David SA. *J Med Chem* 2017;60:2084;
 (b) Liang X, Lv F, Wang B, Yu K, Wu H, Qi Z, Jiang Z, Chen C, Wang A, Miao W, Wang W, Hu Z, Liu J, Liu X, Zhao Z, Wang L, Zhang S, Ye Z, Wang C, Ren T, Wang Y, Liu Q, Liu J. *J Med Chem* 2017;60:1793;
 (c) Odell LR, Abdel-Hamid MK, Hill TA, Chau N, Young KA, Deane FM, Sakoff JA, Andersson S, Daniel JA, Robinson PJ, McCluskey A. *J Med Chem* 2017;60:349;
 (d) Debenham JS, Madsen-Duggan C, Clements MJ, Walsh TF, Kuethe JT, Reibarkh M, Salowe SP, Sonatore LM, Hajdu R, Milligan JA, Visco DM, Zhou D, Lingham RB, Stickens D, DeMartino JA, Tong X, Wolff M, Pang J, Miller RR, Sherer EC, Hale JJ. *J Med Chem* 2016;59:11039;
 (e) Ryu JH, Lee JA, Kim S, Shin YA, Yang J, Han HY, Son HJ, Kim YH, Sa JH, Kim J-S, Lee J, Lee J, Park H-g. *J Med Chem* 2016;59:10176
- [3] (a) Achelle S, Plé N. *Curr Org Synth* 2012;9:163;
 (b) Achelle S, Rodríguez-López J, Robin-le Guen F. *J Org Chem* 2014;79:7564;
 (c) Kato S-i, Yamada Y, Hiyoshi H, Umezumi K, Nakamura Y. *J Org Chem* 2015;80:9076;
 (d) Zhang Z, Xie J, Wang H, Shen B, Zhang J, Hao J, Cao J, Wang Z. *Dyes Pigments* 2016;125:299;
 (e) Achelle S, Rodríguez-López J, Katan C, Robin-le Guen F. *J Phys Chem C* 2016;120:26986;
 (f) Mao M, Zhang X, Zhu B, Wang J, Wu G, Yin Y, Song Q. *Dyes Pigments* 2016;124:72;
 (g) Klikar M, Poul P, Růžička A, Pytela O, Barsella A, Dorkenoo KD, Robin-le Guen F, Bureš F, Achelle S. *J Org Chem* 2017;82:9435.
- [4] Suzuki Y, Sawada J-i, Hibner P, Ishii H, Matsuno K, Sato M, Witulski B, Asai A. *Dyes Pigments* 2017;145:233.
- [5] (a) Gupta AK, Charrette A. *Skinmed* 2015;13:185;
 (b) Barbareschi M, Ital G. *Dermatol. Venereol.* 2018;153:102.
- [6] Mfuh AM, Larionov OV. *Curr Med Chem* 2015;22:2819.
- [7] (a) Katritzky AR, Lagowski JM. *Chemistry of the heterocyclic N-oxides*. New York, N.Y.: Academic Press; 1971;
 (b) Angelo A, Pietra S. *Heterocyclic N-oxides*. Boca Raton, Florida, Inc.: CRC Press; 1991;
 (c) Boykin DW, Balakrishnan P, Baumstark AL. *J Heterocycl Chem* 1985;22:981.
- [8] (a) Sedenkova KN, Averina EB, Grishin YK, Kutateladze AG, Rybakov VB, Kuznetsova TS, Zefirov NS. *J Org Chem* 2012;77:9893;
 (b) Sedenkova KN, Averina EB, Grishin YK, Kuznetsova TS, Zefirov NS. *Tetrahedron Lett* 2014;55:483;
 (c) Sedenkova KN, Averina EB, Grishin YK, Bacunov AB, Troyanov SI, Morozov IV, Deeva EB, Merkulova AV, Kuznetsova TS, Zefirov NS. *Tetrahedron Lett* 2015;56:4927;
 (d) Sedenkova KN, Dueva EV, Averina EB, Grishin YK, Osolodkin DI, Kozlovskaya LI, Palyulin VA, Savelyev EN, Orlinson BS, Novakov IA, Butov GM, Kuznetsova TS, Karganova GG, Zefirov NS. *Org Biomol Chem* 2015;13:3406;
 (e) Sedenkova KN, Averina EB, Grishin Yu K, Kuznetsova TS, Zefirov NS. *Russ Chem Bull* 2016;65:1750;
 (f) Sedenkova KN, Averina EB, Grishin YK, Kolodyazhnaya JV, Rybakov VB, Vasilenko DA, Steglenko DV, Minkin VI, Kuznetsova TS, Zefirov NS. *Tetrahedron Lett* 2017;58:2955;
 (g) Sedenkova KN, Averina EB, Grishin Yu K, Kolodjashnaja JV, Rybakov VB, Kuznetsova TS, Hughes A, Gomes G d P, Alabugin I, Zefirov NS. *Org Biomol Chem* 2017;15:9433;
 (h) Sedenkova KN, Averina EB, Nazarova AA, Grishin Yu K, Karlov DS, Zamoyski VL, Grigoriev VV, Kuznetsova TS, Palyulin VA. *Mendeleev Commun* 2018;28:423;
 (i) Sedenkova KN, Nazarova AA, Khvatov EV, Dueva EV, Orlov AA, Osolodkin DI, Grishin YK, Kuznetsova TS, Palyulin VA, Averina EB. *Mendeleev Commun* 2018;28:592.
- [9] Brouwer AM. *Pure Appl Chem* 2011;83:2213.
- [10] (a) Sheldrick GM. *Acta Crystallogr* 2008;A64:112;
 (b) Sheldrick GM. *Acta Crystallogr* 2015;C71:3;
 (c) Farrugia LJ. *J Appl Crystallogr* 1997;30:568;
 (d) Spek AL. *J Appl Crystallogr* 2003;36:7.
- [11] Niks M, Otto M. *J Immunol Methods* 1990;130:149.
- [12] (a) Orlov AA, Chistov AA, Kozlovskaya LI, Ustinov AV, Korshun VA, Karganova GG, Osolodkin DI. *Med. Chem. Commun.* 2016;7:495;
 (b) Hamilton MA, Russo RC, Thurston RV. *Environ Sci Technol* 1977;11:714.
- [13] For recent examples see.
 (a) Nepomuceno GM, Chan KM, Huynh V, Martin KS, Moore JT, O'Brien TE, Pollo LAE, Sarabia FJ, Tadeus C, Yao Z. *ACS Med Chem Lett* 2015;6:308;
 (b) Reddy BS, Rafeek M, Reddy CVR, Dubey PK. *Heterocycl. Lett.* 2015;5:105;
 (c) Agbo EN, Makhafola TJ, Choong YS, Mphahlele MJ, Ramasami P. *Molecules* 2016;21:28;
 (d) Aliyev TM, Berdnikova DV, Fedorova OA, Gulakova EN, Stremmel C, Ihmels H. *J Org Chem* 2016;81:9075
- [14] (a) Yamanaka H, Ogawa S, Konno S. *Chem Pharm Bull* 1980;28:1526;
 (b) Kövendi A, Kircz M. *Chem Ber* 1965;98:1049;
 (c) Heaney F, Lawless E. *J Heterocycl Chem* 2007;44:569;
 (d) Zimmer R, Lechel T, Rancan G, Bera MK, Reissig H-U. *Synlett* 2010:1793;
 (e) Lewandowska E, Chatfield DC. *Eur J Org Chem* 2005:3297.
- [15] For selected examples see.
 (a) Magoulas GE, Bariamis SE, Athanassopoulos CM, Papaioannou D. *Tetrahedron Lett* 2010;51:1989;
 (b) Muller J-C, Ramuz H. *Helv. Chim. Act.* 1982;65:1445;
 (c) Yamanaka H, Ogawa S, Konno S. *Chem Pharm Bull* 1981;29:98
- [16] (a) Yamanaka H, Sakamoto T, Niitsuma S. *Heterocycles* 1990;31:923;
 (b) Maltese M. *J Org Chem* 1995;60:2436.
- [17] (a) Mei J, Leung NLC, Kwok RTK, Lam JWY, Tang BZ. *Chem Rev* 2015;115:11718;
 (b) Chen J, Liu M, Huang Q, Huang L, Huang H, Deng F, Wen Y, Tian J, Zhang X, Wei Y. *Chem Eng J* 2018;337:82;
 (c) Zhang X, Wang K, Liu M, Zhang X, Tao L, Chen Y, Yen Wei. *Nanoscale* 2015;7:11486;
 (d) Zhang X, Zhang X, Yang B, Liu M, Liu W, Chena Y, Yen Wei. *Polym Chem* 2014;5:356;
 (e) Zhang X, Zhang X, Yang B, Liu M, Liu W, Chena Y, Yen Wei. *Polym Chem* 2014;5:399;
 (f) Huang H, Liu M, Wan Q, Jiang R, Xu D, Huang Q, Wen Y, Deng F, Zhang X, Wei Y. *Mater Sci Eng C* 2018;91:201;
 (g) Jiang R, Liu M, Li C, Huang Q, Huang H, Wan Q, Wen Y, Cao Q-y, Zhanga X, Wei Y. *Mater Sci Eng C* 2017;80:708;
 (h) Chen Z, Zhang J, Song M, Yin J, Yu G-A, Liu Sheng Hua. *Chem Commun* 2015;51:326;
 (i) Chen Z, Liu G, Pu S, Liu SH. *Dyes Pigments* 2017;143:409.
- [18] (a) Yuan L, Lin W, Zheng K, He L, Huang Weimin. *Chem Soc Rev* 2013;42:622;
 (b) Jiang R, Liu M, Huang H, Mao L, Huang Q, Wen Y, Cao Q-y, Tian J, Zhang X, Wei Y. *Dyes Pigments* 2018;151:123;
 (c) Tian J, Jiang R, Gao P, Xu D, Mao L, Zeng G, Liu M, Deng F, Zhang X, Wei Y. *Mater Sci Eng C* 2017;79:563;
 (d) Liu Y, Mao L, Liu X, Liu M, Xu D, Jiang R, Deng F, Li Y, Zhang X, Wei Y. *Mater Sci Eng C* 2017;79:590;
 (e) Jiang R, Liu H, Liu M, Tian J, Huang Q, Huang H, Wen Y, Cao Q-y, Zhanga X, Wei Y. *Mater Sci Eng C* 2017;81:416;
 (f) Jiang R, Liu M, Chen T, Huang H, Huang Q, Tian J, Wen Y, Cao Q-y, Zhang X, Wei Y. *Dyes Pigments* 2018;148:52.